

# Image and noise reduction for assessing driver incompetence in cases of sudden unintended acceleration

Eugene Rhee, Junhee Cho

Department of Electronic Engineering, College of Engineering, Sangmyung University, Cheonan, Republic of Korea

## Article Info

### Article history:

Received Nov 16, 2023

Revised Dec 18, 2023

Accepted Dec 25, 2023

### Keywords:

Camera  
Color recognition  
Image processing  
Noise reduction  
Sudden acceleration

## ABSTRACT

This paper explores using cameras aimed at the accelerator and brake pedals during sudden unintended acceleration in cars, removing noise from captured images to determine driver incompetence. A car model was constructed using Raspberry Pi to simulate brake malfunction using random functions, increasing the revolutions per minute (RPM) to simulate sudden acceleration. By employing a DC encoder motor to measure the motor's rotational speed through waveform counts, the RPM was calculated. The study recognized sudden acceleration when the brake malfunctioned through the DC encoder motor, causing an abnormal RPM increase, allowing camera capture toward the accelerator and brake during sudden acceleration events. Precautions were taken for problems arising from noise in captured images. The Unix operating system was utilized to apply Gaussian filter image processing techniques for noise removal. While using an average value filter led to abrupt changes by replacing with the average of surrounding signals, resulting in an unsmooth image, a Gaussian filter was used in this study to decrease weights as distance from the center increased, mitigating these issues.

*This is an open access article under the [CC BY-SA](https://creativecommons.org/licenses/by-sa/4.0/) license.*



## Corresponding Author:

Junhee Cho

Department of Electronic Engineering, College of Engineering, Sangmyung University

Cheonan, Republic of Korea

Email: [jh\\_cho@smu.ac.kr](mailto:jh_cho@smu.ac.kr)

## 1. INTRODUCTION

As cars become more widespread and their components increasingly electronic, incidents of sudden unintended acceleration in vehicles have been consistently occurring each year. In response, vehicles have been equipped with event data recorders (EDRs) to record accidents [1]-[3]. However, no cases have been acknowledged as due to mechanical faults. Most accidents involving sudden acceleration in cars occur when the revolutions per minute (RPM) increases without the accelerator being pressed and the brakes failing to function. Automotive companies often attribute these accidents to driver error or drowsy driving. Even in legal rulings, the conclusion often favors the automotive companies, citing driver incompetence. Sudden unintended acceleration in cars is a significant accident that can harm not only the driver but also numerous others. Therefore, determining whether it's due to driver incompetence or mechanical faults is crucial. Courts tend to accept the automotive companies' opinion that it's challenging to scientifically prove mechanical faults. Consequently, drivers find themselves in a situation where they must prove it's not due to their incompetence but rather a mechanical fault.

Proving a mechanical fault as a driver can be quite challenging. Consequently, when mechanical faults aren't acknowledged, it often leads to the situation being attributed to driver incompetence, creating an unjust scenario for the driver. Since drivers have to request and acquire evidence from automotive companies

to obtain proof, it puts them at a disadvantage. Therefore, it's crucial for drivers to possess intuitive data regarding their driving competence to avoid unjust situations. Capturing footage with cameras aimed at the accelerator and brake pedals during sudden acceleration incidents provides visual evidence [4]. This footage can then be used to assess the driver's competence. The aim of this research is to empower drivers by providing them with evidence to assess their own driving competence, ultimately preventing unjust situations.

In this paper, we simulate sudden acceleration incidents using Raspberry Pi. Upon detecting such an event, we identify it as a case of sudden acceleration. During this scenario, cameras are directed towards the accelerator and brake pedals to capture footage for assessing the driver's competence. Subsequently, we conducted research on a program that utilizes Gaussian filter image processing techniques to remove noise from the captured images.

## 2. SIMULATING SUDDEN ACCELATION ACCIDENTS

### 2.1. RAND function

RAND function is a programming function used to generate random numbers. Essentially, it's used for creating random numbers or randomization within a program. Typically, the RAND function generates random numbers starting from 0. When used as "rand() % 10", it generates numbers from 0 to 9. This method allows for controlling the range of random number generation [5], [6]. In C programming, to use the RAND function, we need to include the "stdlib.h" header file.

### 2.2. Algorithm for sudden acceleration accidents

Sudden acceleration in cars occurs when the RPM suddenly increases, and the brakes fail to function. In Figure 1, using the rand function, we simulated a situation where a brake malfunction was induced to create a sudden acceleration scenario. When a brake malfunction was introduced, the RPM was increased to simulate the sudden acceleration. When the brakes functioned normally, they were ensured to operate correctly. This study proceeded with a 20% probability of brake malfunction occurrence.

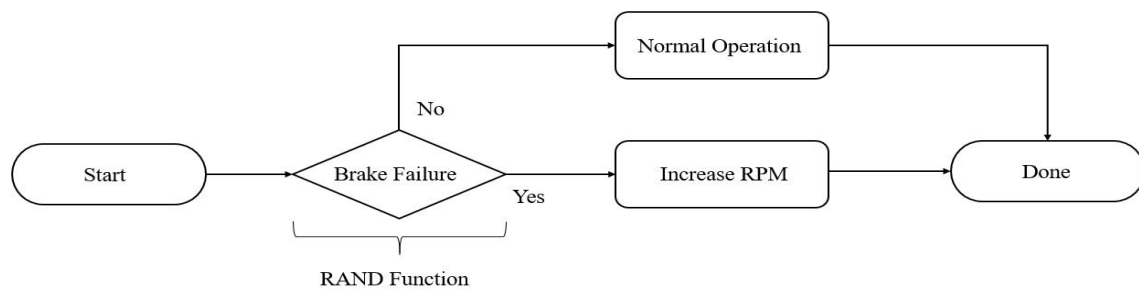


Figure 1. Flow chart for sudden acceleration accidents

## 3. RECOGNITION OF SUDDEN ACCELERATION INCIDENTS

### 3.1. DC encoder motor

The Incremental method of a DC encoder motor involves light emitted from light emitting diodes (LEDs) in Figure 2, shining onto phases A, B, and Z. As the encoder rotates, the light passing through the slits is alternately obstructed and allowed to pass through each phase [7], [8]. This method measures the rotational speed of the shaft by how the emitted light interacts with and is obscured by the rotation slits. A crucial aspect of encoders is their resolution. Higher resolution allows for finer measurement of the rotational speed. The signals generated by the encoder per one full rotation are determined by the resolution. For instance, with a resolution of 60, 60 pulses are produced per one complete rotation. This translates to  $60/360 = 1/6^\circ$ , resulting in one pulse per  $1/6^\circ$  of movement. The encoder's rotational angular velocity is measured in a given period, forming the basis for RPM measurement. In this study, RPM is measured as depicted in Figure 2, and this data is used to calculate velocity [9].

### 3.2. Algorithm for recognizing sudden acceleration

Sudden acceleration in a car occurs when the RPM and speed increase abruptly while the brakes fail to engage. Hence, as depicted in Figure 3, if the brakes are applied but fail to function while the RPM

increases, it's identified as a case of sudden acceleration in the vehicle. This study utilizes a DC encoder motor to measure RPM and thereby recognizes the increase in RPM.

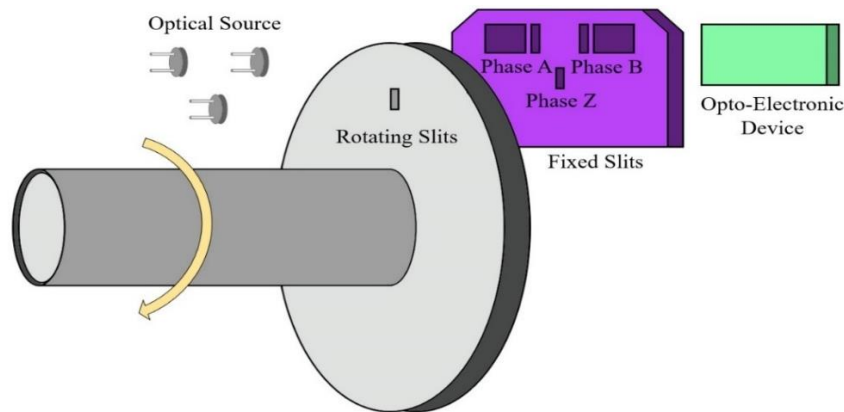


Figure 2. Incremental method of DC encoder motor

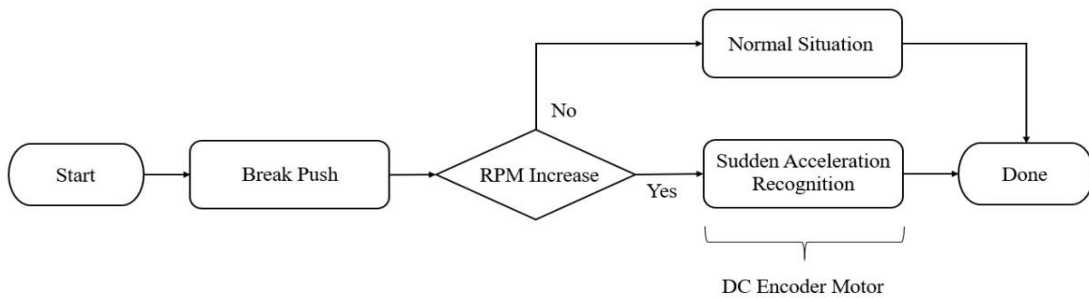


Figure 3. Flow chart for recognizing sudden acceleration

**4. USING CAMERAS DURING SUDDEN ACCELERATION**

Figure 4 implements and recognizes sudden acceleration scenarios based on brake engagement. Upon recognizing a sudden acceleration event in the vehicle, cameras are directed towards the accelerator and brake pedals. To accommodate nighttime driving, camera lighting is utilized. The camera lighting is activated before capturing footage and turned off once the recording ends. The filenames for the captured footage are based on the time of the sudden acceleration event. This study employs the localtime function to set filenames based on time, preventing file duplication and recording the time of the sudden acceleration event.

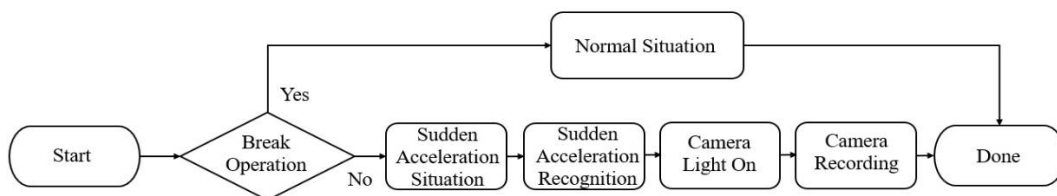


Figure 4. Flow chart for camera recording

**5. NOISE REDUCTION**

**5.1. Noise**

Noise refers to unwanted signals or unintended data, arising from interference or undesired distortions within the dataset [10]-[12]. In the case of image sensors, it occurs due to technical factors and external

influences, leading to irregularities in the images [13]. Noise can originate from various factors, primarily from prolonged exposure and high sensitivity. Types of noise include Gaussian noise [14]-[16], Salt and Pepper noise [17]-[19], uniform noise [20]-[22], photon noise [23]-[25], readout noise [26]-[28], reset noise [29]-[31], quantization noise [32]-[34], and more [35]-[37]. To mitigate such noise, noise filters are employed.

**5.2. Gaussian filter**

The Gaussian filter processes pixel values by computing a weighted average of neighboring pixel values, effectively removing noise. This is obtained through the Gaussian function. Due to its detailed removal, it results in a smoother image, also known as smoothing. In (1), when  $\sigma$  is small, the height increases, and the width decreases, allowing fewer low-frequency components to pass through [38]-[40]. Conversely, when  $\sigma$  is large, the height decreases, and the width increases, enabling more low-frequency components to pass through. Adjusting  $\sigma$  allows control over the amount of low and high-frequency content. As  $\sigma$  increases, the blurring effect intensifies [41]-[43]. Blurring involves passing through a low-pass filter, eliminating high-frequency components such as the image's contours, resulting in a smoother image. Gaussian filters render weight values nearly insignificant when the  $\sigma$  size is 3 or less or greater than -3.

$$G(x) = \frac{1}{\sqrt{2\pi}\sigma} e^{-\frac{x^2+y^2}{2\sigma^2}} \tag{1}$$

**5.3. Mean filter**

The mean filter determines pixel values by computing the arithmetic mean of neighboring pixel values. It's a form of arithmetic mean filter, replacing the central pixel value with the calculated average of the image pixel values [44], [45]. This filter computes the mean of selected neighboring pixel values by summing up the values and dividing by the number of nearby pixels. The computed average value substitutes the central pixel value. Consequently, it reduces variations between pixels, blurring edges, and reducing noise in the image [46]. However, excessive use can cause blurring at object boundaries, making object recognition challenging. The mean filter typically utilizes a  $3 \times 3$  mask or a  $5 \times 5$  mask. Larger masks result in smoother images.

**5.4. Image convolution**

Image convolution is a technique used in digital image processing and computer vision. It involves transforming or enhancing images using filters or kernels [47], [48]. Image convolution performs operations between each pixel of an image and its neighboring pixels. It is also referred to as image filtering or convolution operation. Convolution involves multiplying each pixel of an image with its neighboring pixels and summing up the resulting values. Image rotation utilizes not only filters but also extracts high-frequency and low-frequency components, used in tasks like image pyramids creation, deep learning, and convolutional neural networks. The Gaussian filter can also be applied using image convolution. Typically, Gaussian filters, shown in Figure 5, use masks of sizes like  $3 \times 3$ ,  $5 \times 5$ , or  $7 \times 7$ . As the mask size increases, the image becomes smoother but requires more computations, thus taking longer processing time [49], [50]. In other words, a larger mask size increases the blurring effect while slowing down processing speed. In the code, the reason for  $y < YY - 4$ ,  $x < XX - 4$  is as follows: a  $7 \times 7$  image undergoes image convolution three times using a  $5 \times 5$  mask, hence subtracting 4 from both the horizontal and vertical sizes. Figure 5 demonstrates an image after applying the Gaussian filter through image convolution.

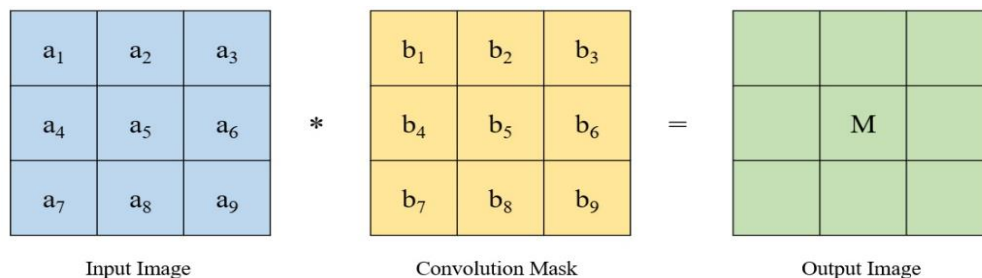


Figure 5. Image convolution

**5.5. FFmpeg**

In this paper, noise reduction was performed on videos rather than photos. The videos are structured similarly to Figure 5, with no information on width, height, or maximum luminance. For this reason, FFmpeg

was utilized in this research. FFmpeg is a library or tool capable of handling various multimedia file operations such as decoding, encoding, conversion, and streaming for audio, video, and more. Therefore, video processing or conversion tasks were executed using FFmpeg. Various options of FFmpeg were set using commands. Table 1 highlights some key options. The structure of FFmpeg commands follows the pattern 'ffmpeg [options] -i input output'. There is a range of options available within FFmpeg, which are used together to perform video processing and conversion tasks. In this study, the Gaussian filter was applied using FFmpeg commands.

Table 1. Main options of FFmpeg

Option	Function
-i	Specifies the input file
-f	Specifies the output file format
-r	Sets the video frame rate
-s	Specifies the video resolution
-b	Sets the bitrate
-codec:a, -codec:v	Specifies audio and video codecs
-ss, -t	Specifies the time range to be used from the input file
-filter_complex	Applies filter graph
map	Selects streams from the input file to be used in the output

## 6. RESULTS

Using the rand function, a brake malfunction is implemented with a 20% probability. When a brake malfunction occurs, the RPM is increased, simulating a sudden acceleration situation. Continuously measuring RPM using the DC encoder motor, if the RPM measured after pressing the brake does not decrease but rather increases, it's identified as a sudden acceleration event in the car. Upon recognizing the sudden acceleration event, the camera initiates recording towards the accelerator and brake. Preventing duplicate file names using the localtime function, timestamps in file names record the time of the sudden acceleration incident. The recorded video's noise is removed using a Gaussian filter. As mentioned before, distinguishing whether the driver pressed the accelerator or the brake during a sudden acceleration event enables assessment of the driver's proficiency behind the wheel.

## 7. CONCLUSION

This research utilized C language functions such as rand and localtime, alongside a DC encoder motor and Gaussian filter for image processing. The rand function was employed to simulate sudden acceleration, while the DC encoder motor recognized and recorded instances of sudden acceleration. When a sudden acceleration event occurred, the program captured the driver's reaction. The use of localtime for file naming prevented duplicates and recorded the accident time. Additionally, noise reduction using a Gaussian filter notably improved the outcomes.

## ACKNOWLEDGEMENTS

This research was funded by a 2023 research Grant from Sangmyung University(2023-A000-0081).

## REFERENCES




- [1] Y. Yao and E. Atkins, "The smart black box: A value-driven high-bandwidth automotive event data recorder," *IEEE Transactions on Intelligent Transportation Systems*, vol. 22, no. 3, pp. 1484-1496, Mar. 2021, doi: 10.1109/TITS.2020.2971385.
- [2] M. Siami, M. Naderpour, and J. Lu, "A mobile telematics pattern recognition framework for driving behavior extraction," *IEEE Transactions on Intelligent Transportation Systems*, vol. 22, no. 3, pp. 1459-1472, Mar. 2021, doi: 10.1109/TITS.2020.2971214.
- [3] J. M. Scanlon, R. Sherony, and H. C. Gabler, "Models of driver acceleration behavior prior to real-world intersection crashes," *IEEE Transactions on Intelligent Transportation Systems*, vol. 19, no. 3, pp. 774-786, Mar. 2018, doi: 10.1109/TITS.2017.2699079.
- [4] K. Takeda *et al.*, "Self-coaching system based on recorded driving data: learning from one's experiences," *IEEE Transactions on Intelligent Transportation Systems*, vol. 13, no. 4, pp. 1821-1831, Dec. 2012, doi: 10.1109/TITS.2012.2205917.
- [5] Y. Li, Q. He, and R. S. Blum, "On the product of two correlated complex gaussian random variables," *IEEE Signal Processing Letters*, vol. 27, pp. 16-20, 2020, doi: 10.1109/LSP.2019.2953634.
- [6] S. Nadarajah and S. Kotz, "Exact distribution of the max/min of two gaussian random variables," *IEEE Transactions on Very Large Scale Integration (VLSI) System*, vol. 16, no. 2, pp. 210-212, Feb. 2008, doi: 10.1109/TVLSI.2007.912191.
- [7] S. Lu, Y. Qin, J. Hang, B. Zhang, and Q. Wang, "Adaptively estimating rotation speed from DC motor current ripple for order tracking and fault diagnosis," *IEEE Transactions on Instrumentation and Measurement*, vol. 68, no. 3, pp. 741-753, Mar. 2019, doi: 10.1109/TIM.2018.2852978.

- [8] J. N. Nash, "Direct torque control, induction motor vector control without an encoder," *IEEE Transactions on Industry Applications*, vol. 33, no. 2, pp. 333-341, Mar. 1997, doi: 10.1109/28.567792.
- [9] J. Fang, X. Zhou, and G. Liu, "Precise accelerated torque control for small inductance brushless DC motor," *IEEE Transactions on Power Electronics*, vol. 28, no. 3, pp. 1400-1412, Mar. 2013, doi: 10.1109/TPEL.2012.2210251.
- [10] H. Zhu and M. K. Ng, "Structured dictionary learning for image denoising under mixed gaussian and impulse noise," *IEEE Transactions Image Process*, vol. 29, pp. 6680-6693, May. 2020, doi: 10.1109/TIP.2020.2992895.
- [11] D. -Q. Chen and L.-Z. Cheng, "Spatially adapted total variation model to remove multiplicative noise," *IEEE Transactions Image Process*, vol. 21, no. 4, pp. 1650-1662, Apr. 2012, doi: 10.1109/TIP.2011.2172801.
- [12] G. Liu, H. Zhong and L. Jiao, "Comparing noisy patches for image denoising: a double noise similarity model," *IEEE Transactions Image Process*, vol. 24, no. 3, pp. 862-872, Mar. 2015, doi: 10.1109/TIP.2014.2387390.
- [13] A. Singh, G. Sethi, and G. S. Kalra, "Spatially adaptive image denoising via enhanced noise detection method for grayscale and color images," *IEEE Access*, vol. 8, pp. 112985-113002, Jun. 2020, doi: 10.1109/ACCESS.2020.3003874.
- [14] N. Bähler, M. E. Helou, É. Objois, K. Okumuş, and S. Süsstrunk, "PoGalN: Poisson-gaussian image noise modeling from paired samples," *IEEE Signal Processing Letters*, vol. 29, pp. 2602-2606, Dec. 2022, doi: 10.1109/LSP.2022.3227522.
- [15] M. Rakhshanfar and M. A. Amer, "Estimation of gaussian, poissonian-gaussian, and processed visual noise and its level function," *IEEE Transactions Image Process*, vol. 25, no. 9, pp. 4172-4185, Sept. 2016, doi: 10.1109/TIP.2016.2588320.
- [16] M. Naseri and N. C. Beaulieu, "Fast simulation of additive generalized gaussian noise environments," *IEEE Communications Letters*, vol. 24, no. 8, pp. 1651-1654, Aug. 2020, doi: 10.1109/LCOMM.2020.2989246.
- [17] M. Monajati and E. Kabir, "A modified inexact arithmetic median filter for removing salt-and-pepper noise from gray-level images," *IEEE Transactions on Circuits and Systems II: Express Briefs*, vol. 67, no. 4, pp. 750-754, Apr. 2020, doi: 10.1109/TCSII.2019.2919446.
- [18] V. Singh, R. Dev, N. K. Dhar, P. Agrawal and N. K. Verma, "Adaptive type-2 fuzzy approach for filtering salt and pepper noise in grayscale images," *IEEE Transactions on Fuzzy Systems*, vol. 26, no. 5, pp. 3170-3176, Oct. 2018, doi: 10.1109/TFUZZ.2018.2805289.
- [19] S. N. Sulaiman and N. A. M. Isa, "Denoising-based clustering algorithms for segmentation of low level salt-and-pepper noise-corrupted images," *IEEE Transactions on Consumer Electronics*, vol. 56, no. 4, pp. 2702-2710, Nov. 2010, doi: 10.1109/TCE.2010.5681159.
- [20] J. D. Alves and G. Evans, "Digital pseudorandom uniform noise generators for ADC histogram test," in *Conference on Design of Circuits and Integrated Systems (DCIS)*, Nov. 2015, pp. 1-6, doi: 10.1109/DCIS.2015.7388592.
- [21] G. Evans, J. Goes, A. Steiger-Garcão, M. D. Ortigueira, N. Paulino, and J. S. Lopes, "Low-voltage low-power CMOS analogue circuits for Gaussian and uniform noise generation," in *IEEE International Symposium on Circuits and Systems (ISCAS)*, May. 2003, pp. I-1, doi: 10.1109/ISCAS.2003.1205521.
- [22] X. Liu, Z. Chen, and Y. W. Wen, "A dual method for uniform noise removal base on L [infinity] norm constraint," in *Proceedings 4<sup>th</sup> International Conference Information Science and Control Engineering (ICISCE)*, Jul. 2017, pp. 1346-1350, doi: 10.1109/ICISCE.2017.280.
- [23] J. Rapp and V. K. Goyal, "A few photons among many: unmixing signal and noise for photon-efficient active imaging," *IEEE Transactions on Computational Imaging*, vol. 3, no. 3, pp. 445-459, Sept. 2017, doi: 10.1109/TCI.2017.2706028.
- [24] D. Leviski, M. Wány, and B. Choubey, "Compensation of signal-dependent readout noise in photon transfer curve characterisation of CMOS image sensors," *IEEE Transactions on Circuits and Systems II: Express Briefs*, vol. 68, no. 1, pp. 102-105, Jan. 2021, doi: 10.1109/TCSII.2020.3010366.
- [25] G. Zhang *et al.*, "A noise-removal algorithm without input parameters based on quadtree isolation for photon-counting LiDAR," *IEEE Geoscience and Remote Sensing Letters*, vol. 19, pp. 1-5, Jun. 2022, Art no. 6501905, doi: 10.1109/LGRS.2021.3081721.
- [26] H. Wang, H. Chen, X. Kong, M. Wang, Y. Zhang, and X. Xie, "Study on noise matching between SQUID sensor and its readout electronics," *IEEE Transactions on Applied Superconductivity*, vol. 27, no. 4, pp. 1-4, Jun. 2017, Art no. 1601104, doi: 10.1109/TASC.2016.2631430.
- [27] Y. Degerli, F. Lavernhe, P. Magnan, and J. A. Farre, "Analysis and reduction of signal readout circuitry temporal noise in CMOS image sensors for low-light levels," *IEEE Transactions on Electron Devices*, vol. 47, no. 5, pp. 949-962, May. 2000, doi: 10.1109/16.841226.
- [28] A. Boukhayma, A. Peizerat, and C. Enz, "Temporal readout noise analysis and reduction techniques for low-light CMOS image sensors," *IEEE Transactions Electron Devices*, vol. 63, no. 1, pp. 72-78, Jan. 2016, doi: 10.1109/TED.2015.2434799.
- [29] J. Lai and A. Nathan, "Reset and partition noise in active pixel image sensors," *IEEE Transactions Electron Devices*, vol. 52, no. 10, pp. 2329-2332, Oct. 2005, doi: 10.1109/TED.2005.856192.
- [30] J. Hynccek, "Spectral analysis of reset noise observed in CCD charge-detection circuits," *IEEE Transactions Electron Devices*, vol. 37, no. 3, pp. 640-647, Mar. 1990, doi: 10.1109/16.47768.
- [31] B. Fowler, M. D. Godfrey, and S. Mims, "Reset noise reduction in capacitive sensors," *IEEE Transactions on Circuits and Systems I: Regular Papers*, vol. 53, no. 8, pp. 1658-1669, Aug. 2006, doi: 10.1109/TCSI.2006.877890.
- [32] L. Feng, W. Rhee, and Z. Wang, "A quantization noise reduction method for delta-sigma fractional-N PLLs using cascaded injection-locked oscillators," *IEEE Transactions on Circuits and Systems II: Express Briefs*, vol. 69, no. 5, pp. 2448-2452, May. 2022, doi: 10.1109/TCSII.2022.3161063.
- [33] G. Chiorboli, G. Franco and C. Morandi, "Uncertainties in quantization-noise estimates for analog-to-digital converters," *IEEE Transactions on Instrumentation and Measurement*, vol. 46, no. 1, pp. 56-60, Feb. 1997, doi: 10.1109/19.552157.
- [34] C. Venerus and I. Galton, "Quantization noise cancellation for FDC-based fractional- N PLLs," *IEEE Transactions on Circuits and Systems II: Express Briefs*, vol. 62, no. 12, pp. 1119-1123, Dec. 2015, doi: 10.1109/TCSII.2015.2468913.
- [35] V. Patanavijit and K. Thakulsukanant, "A computational experimental of noise suppressing technique stand on hard decision threshold dissimilarity," *Indonesian Journal of Electrical Engineering and Computer Science (IJECS)*, vol. 24, no. 1, pp. 144-156, Oct. 2021, doi: 10.11591/ijeecs.v24.i1.pp144-156.
- [36] S. Thomas and A. Krishna, "Impulse noise recuperation from grayscale and medical images using supervised curve fitting linear regression and mean filter," *Indonesian Journal of Electrical Engineering and Computer Science (IJECS)*, vol. 28, no. 2, pp. 777-786, Nov. 2022, doi: 10.11591/ijeecs.v28.i2.pp777-786.
- [37] A. A. Hussein, S. A. Hussain, and A. H. Reja, "Image mixed gaussian and impulse noise elimination based on sparse representation model," *Indonesian Journal of Electrical Engineering and Computer Science (IJECS)*, vol. 23, no. 3, pp. 1440-1450, Sept. 2021, doi: 10.11591/ijeecs.v23.i3.pp1440-1450.
- [38] B. Jia and M. Xin, "Data-driven enhanced nonlinear gaussian filter," *IEEE Transactions on Circuits and Systems II: Express Briefs*, vol. 67, no. 6, pp. 1144-1148, Jun. 2020, doi: 10.1109/TCSII.2019.2926657.




- [39] A. Mohammadi and K. N. Plataniotis, "Complex-valued gaussian sum filter for nonlinear filtering of non-gaussian/non-circular noise," *IEEE Signal Processing Letters*, vol. 22, no. 4, pp. 440-444, Apr. 2015, doi: 10.1109/LSP.2014.2361459.
- [40] T. D. Pham, "Estimating parameters of optimal average and adaptive wiener filters for image restoration with sequential gaussian simulation," *IEEE Signal Processing Letters*, vol. 22, no. 11, pp. 1950-1954, Nov. 2015, doi: 10.1109/LSP.2015.2448732.
- [41] K. Zhao, P. Li, and S.-M. Song, "Gaussian filter for nonlinear stochastic uncertain systems with correlated noises," *IEEE Sensors Journal*, vol. 18, no. 23, pp. 9584-9594, 1 Dec.1, 2018, doi: 10.1109/JSEN.2018.2865620.
- [42] N. Yongfang and Z. Tao, "Improved pruning algorithm for Gaussian mixture probability hypothesis density filter," *Journal of Systems Engineering and Electronics*, vol. 29, no. 2, pp. 229-235, Apr. 2018, doi: 10.21629/JSEE.2018.02.02.
- [43] R. Cheng, L. Xia, Y. Ran, J. Rohollahnejad, J. Zhou, and Y. Wen, "Interrogation of ultrashort bragg grating sensors using shifted optical Gaussian filters," *IEEE Photonics Technology Letters*, vol. 27, no. 17, pp. 1833-1836, 2015, doi: 10.1109/LPT.2015.2443812.
- [44] X. Wang, "An estimation on the output mean value of median filtering at edge location," *IEEE Transactions on Signal Processing*, vol. 47, no. 11, pp. 3149-3152, Nov. 1999, doi: 10.1109/78.796452.
- [45] J.-M. Valin and I. B. Collings, "Interference-normalized least mean square algorithm," *IEEE Signal Processing Letters*, vol. 14, no. 12, pp. 988-991, Dec. 2007, doi: 10.1109/LSP.2007.908017.
- [46] K. B. Khan, A. A. Khaliq, M. Shahid, and H. Ullah, "Poisson noise reduction in scintigraphic images using gradient adaptive trimmed mean filter," in *Proc. International Conference Intelligent Systems Engineering (ICISE)*, Jan. 2016, pp. 301-305, doi: 10.1109/INTELSE.2016.7475138.
- [47] J. Jonsson, B. L. Cheeseman, S. Maddu, K. Gonciarz, and I. F. Sbalzarini, "Parallel discrete convolutions on adaptive particle representations of images," *IEEE Transactions on Image Processing*, vol. 31, pp. 4197-4212, Jun. 2022, doi: 10.1109/TIP.2022.3181487.
- [48] L. Guo, Z. Zha, S. Ravishankar, and B. Wen, "Exploiting non-local priors via self-convolution for highly-efficient image restoration," *IEEE Transactions on Image Processing*, vol. 31, pp. 1311-1324, Jan. 2022, doi: 10.1109/TIP.2022.3140918.
- [49] C.-C. Lin, M.-H. Sheu, C. Liaw, and H.-K. Chiang, "Fast first-order polynomials convolution interpolation for real-time digital image reconstruction," *IEEE Transactions on Circuits and Systems for Video Technology (TCSVT)*, vol. 20, no. 9, pp. 1260-1264, Sept. 2010, doi: 10.1109/TCSVT.2010.2057017.
- [50] G. Liu *et al.*, "Partial convolution for padding, inpainting, and image synthesis," *IEEE Transactions on Pattern Analysis and Machine Intelligence*, vol. 45, no. 5, pp. 6096-6110, 1 May 2023, doi: 10.1109/TPAMI.2022.3209702.

## BIOGRAPHIES OF AUTHORS



**Eugene Rhee**    received the Ph.D. degree in electronics from Hanyang University, Korea, in 2010. He was a visiting professor at Chuo University, Japan from 2010 to 2011. Since 2012, he has been with Sangmyung University, Korea, where he is currently an associate professor in the Department of Electronic Engineering. His research area includes microwave, electromagnetic compatibility, electromagnetic interference, and reverberation chamber. He can be contacted at email: eugenerhee@smu.ac.kr.



**Junhee Cho**    received his Ph.D. degree in electrical engineering from University of Cambridge, U.K. in 2017. Since 2020, he has been an Assistant Professor in the department of electronics engineering, Sangmyung University, Republic of Korea. His current research interests include nanophotonics-based secure communications. He can be contacted at email: jh\_cho@smu.ac.kr.